Batteries & Supercaps

Supporting Information

Cost-Effective Vat Orange 3-Derived Organic Cathodes for Electrochemical Energy Storage

Ling Chen,[a] Fangfang Xing,[a] Qiting Lin,[a] Ahsan Waqas,[a] Xiujuan Wang,[a] Thomas Baumgartner,*[b] Xiaoming He*[a]

[a] L. Chen, F. Xing, Q. Lin, A. Waqas, Dr. X. Wang, Prof. Dr. X. He
Key Laboratory of Applied Surface and Colloid Chemistry (Ministry of Education), School of Chemistry and Chemical Engineering
Shaanxi Normal University
Xi'an 710119, P.R. China
E-mail: xmhe@snnu.edu.cn

[b] Prof. Dr. T. Baumgartner
Department of Chemistry
York University
Toronto Ontario M3J 1P3, Canada
E-mail: tbaumgar@yorku.ca

Calculations of the Electrochemical Metrics

Theoretical capacity (C_{theor}, mAh g^{-1}) was calculated according to the equation S1:

$$C_{theor} = \frac{nF}{3.6 \times M} \qquad \text{(S1)}$$

where n is the number of electrons transferred per molecules (for small molecules) or repeating structure unit (for polymers), F is the Faraday's constant (96500 C mol^{-1}), M is molecular weight of the molecules (for small molecules) or repeating unit (for polymers).

Degree of polymerization (DP) of PATS: DP of **PATS** was estimated by elemental analysis (EA). The general structure and EA result of PATS are shown below:

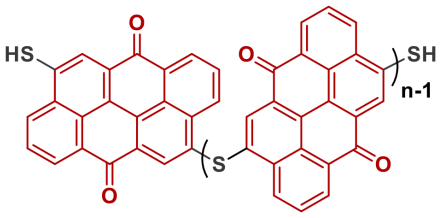

Elemental Analysis result

C	H	S	Weight ratio of C/S (wt%/wt%)
69.75	3.491	11.71	5.96

Table S1. The carbon to sulfur weight ratio of the polymer material with different degrees of polymerization.

DP (n)	Weight ratio C/S (wt%/wt%)
1	4.12
2	5.49
3	6.18
4	6.59

As described in Table S1, the carbon-to-sulfur weight ratio (C/S, wt%/wt%) of the polymer material is dependent on the degree of polymerization (n). The elemental analysis demonstrates that the prepared polymer material contains 69.75% of carbon element and 11.71% of sulfur, with a C/S ratio of 5.96. The C/S ratio is close to 6.18 for the trimer. The result demonstrates that the prepared polymer is mainly comprised of trimer (n = 3). However, the existence of polymer with higher (or lower) degree of polymerization cannot be excluded.

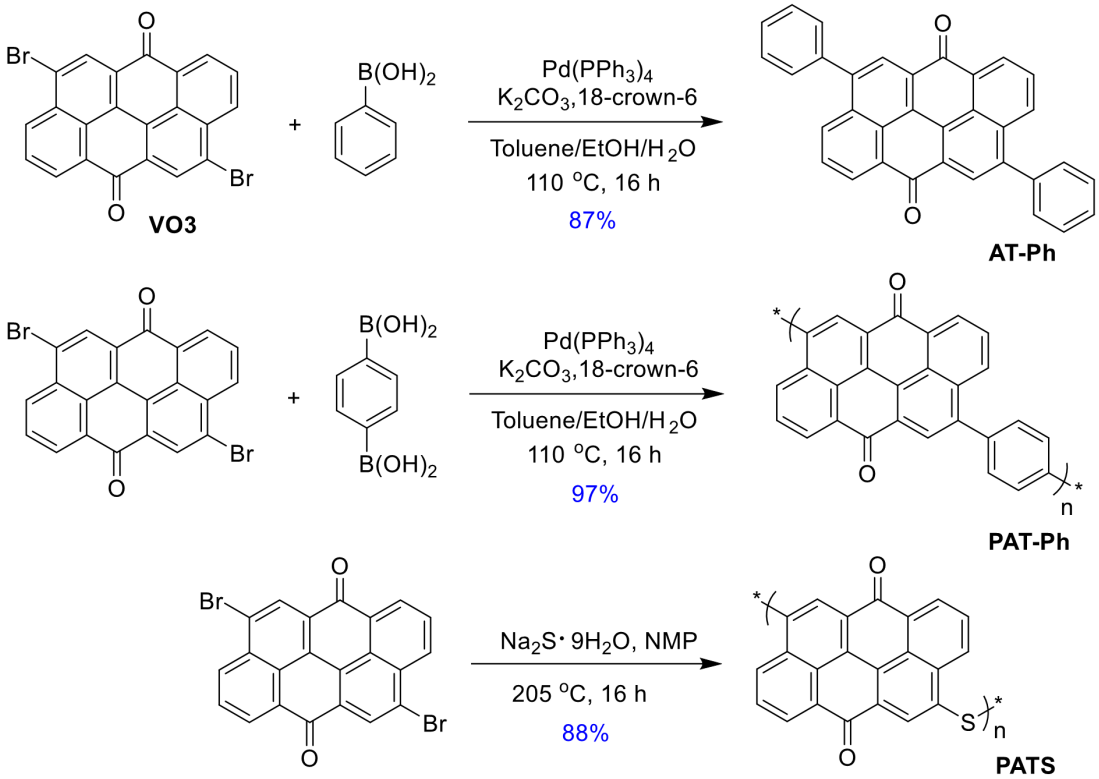

Scheme S1. Synthetic routes toward **AT-Ph, PAT-Ph** and **PATS**.

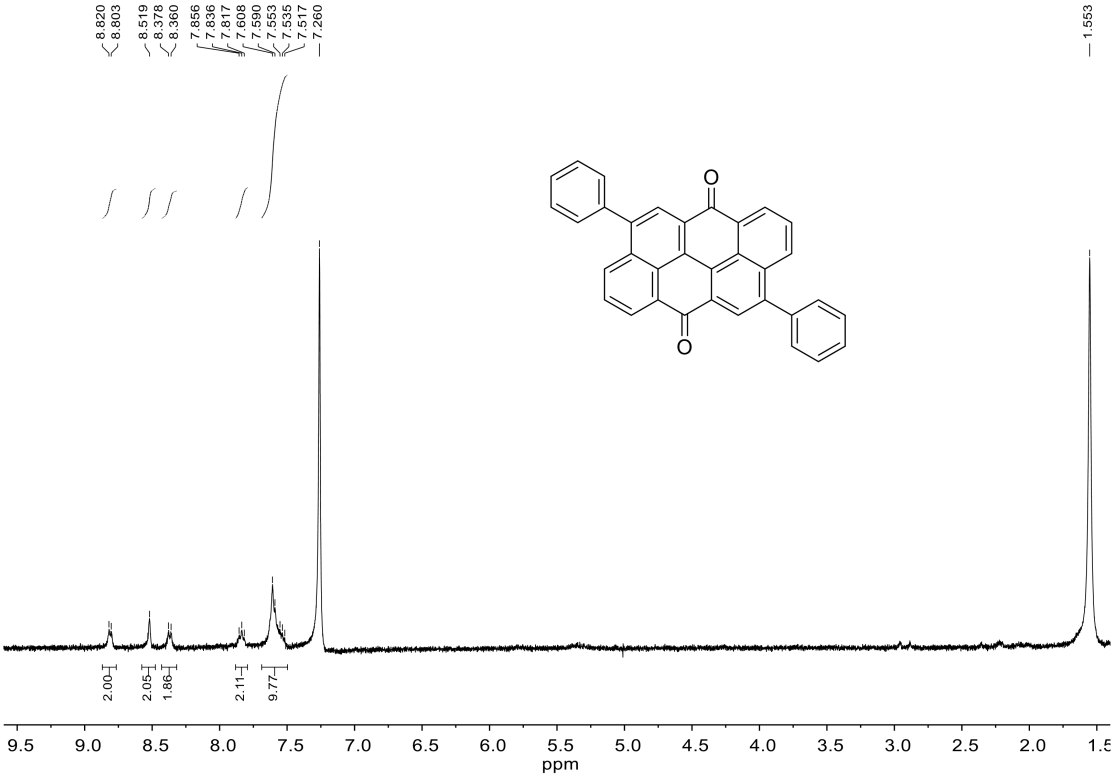

Figure S1. ^{1}H NMR spectrum of **AT-Ph** in $CDCl_3$ at 298 K.

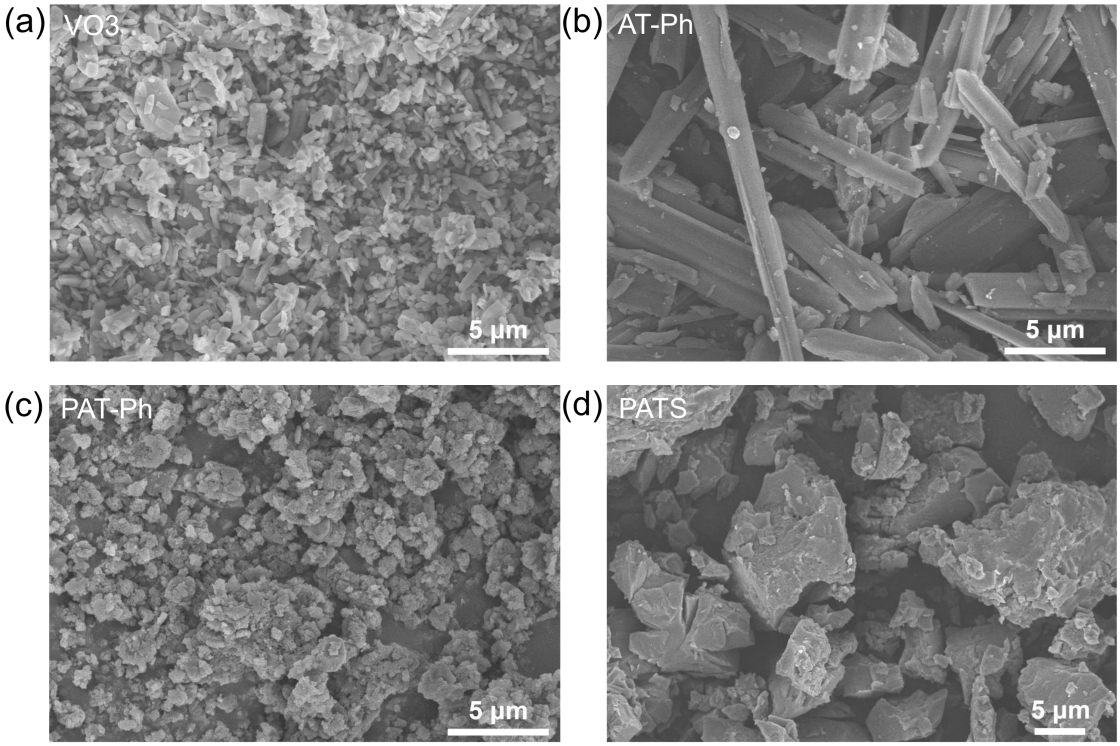

Figure S2. SEM images of **VO3** (a), **AT-Ph** (b), **PAT-Ph** (c), and **PATS** (d).

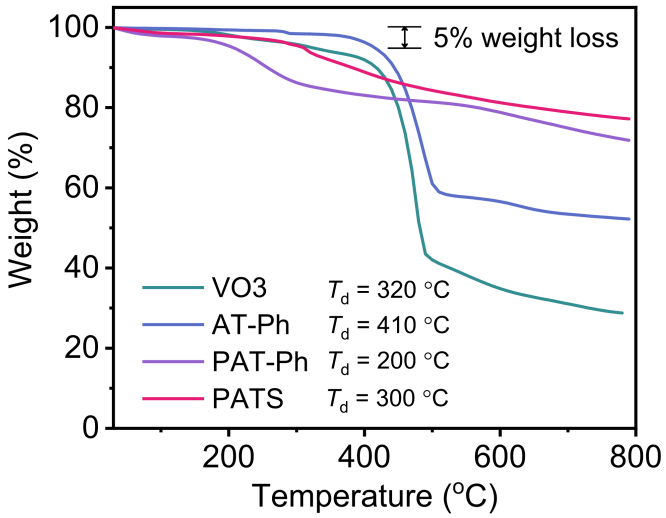

Figure S3. TGA of **VO3, AT-Ph, PAT-Ph** and **PATS**.

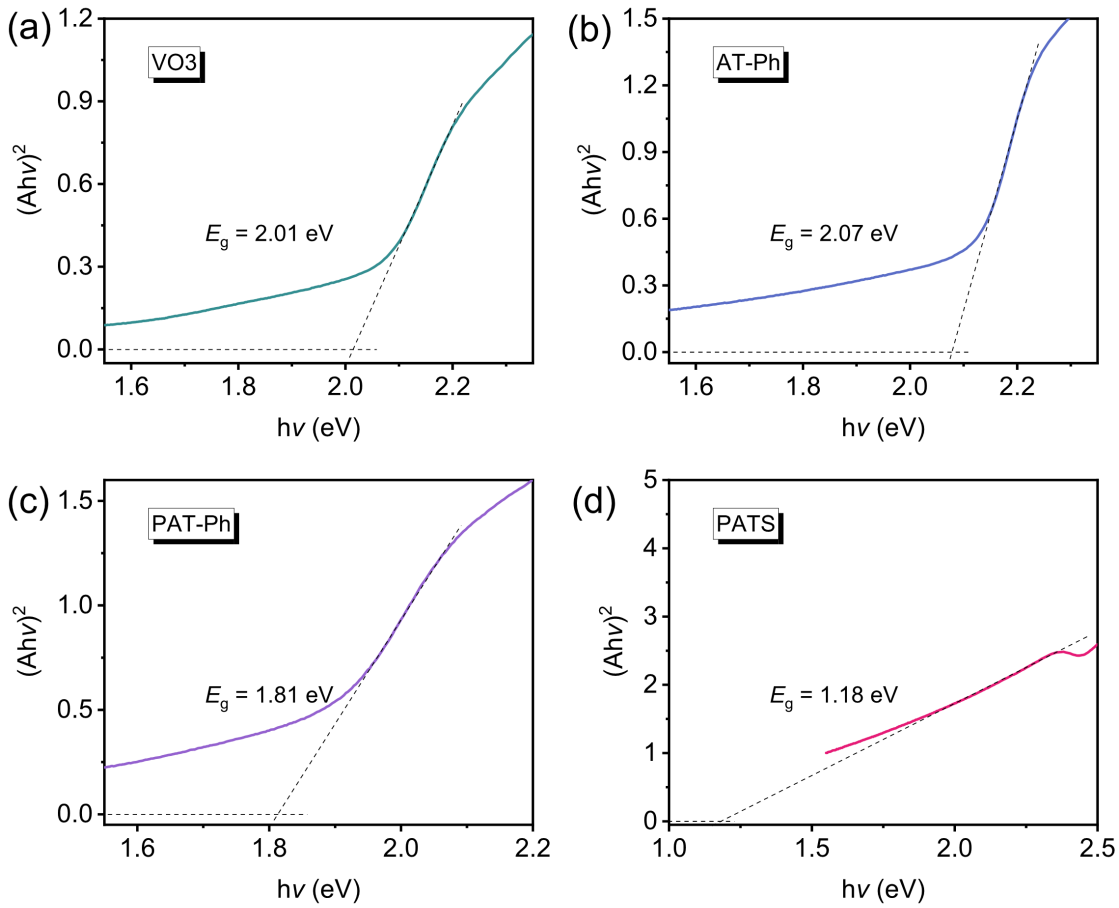

Figure S4. Tauc plots of the diffuse reflectance UV–vis absorption spectra for the (a) **VO3**, (b) **AT-Ph**, (c) **PAT-Ph** and (d) **PATS**. The intersection of two dashed lines indicates the value of estimated optical bandgap.

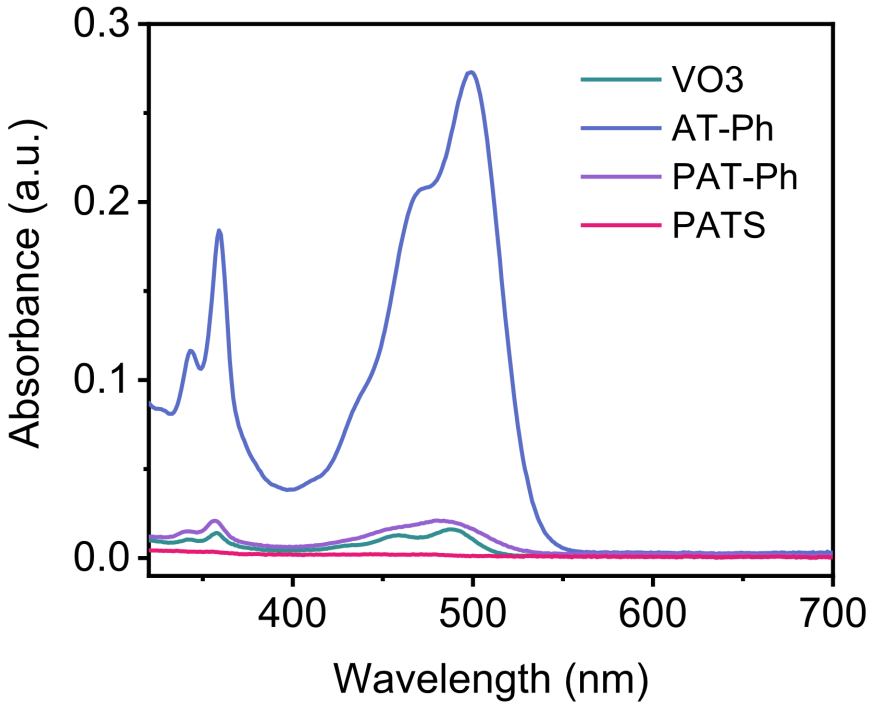

Figure S5. UV-vis spectra of **VO3**, **AT-Ph**, **PAT-Ph** and **PATS** in G4 (tetraglyme). The sample was soaked in G4 for three days before measurement.

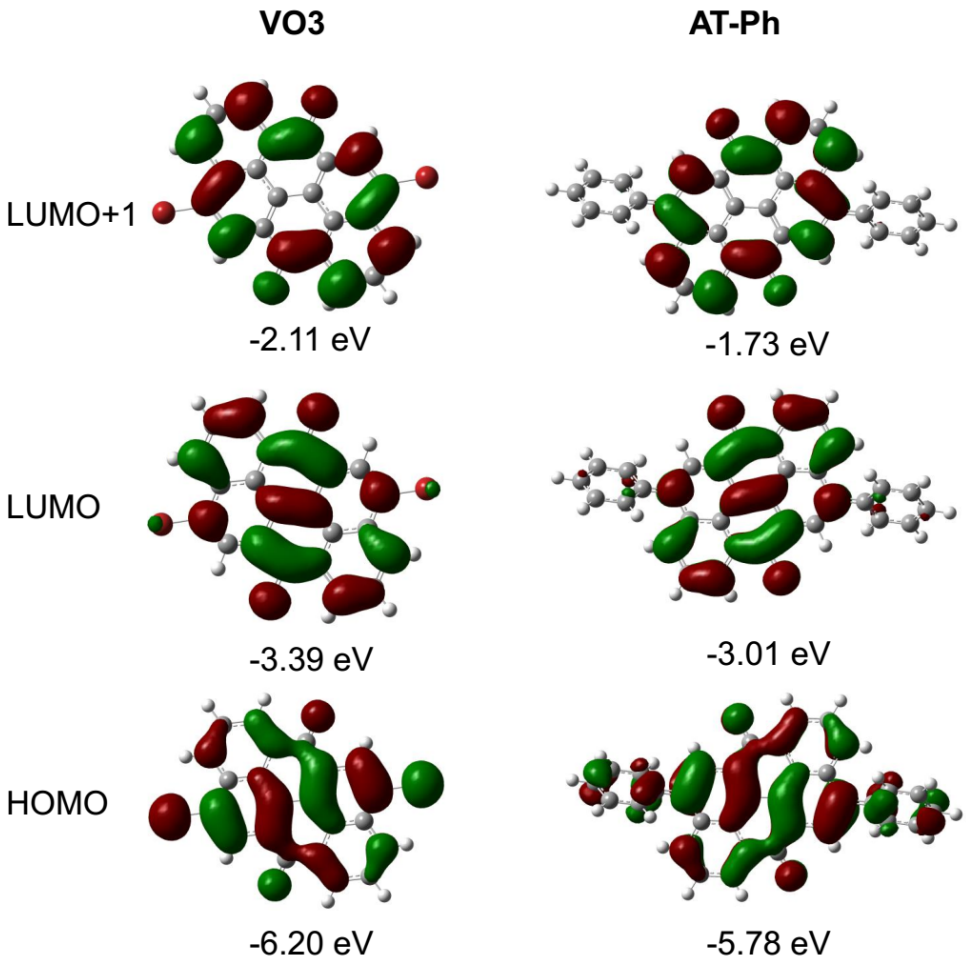

Figure S6. Frontier molecular orbital diagrams for **VO3** and **AT-Ph** (B3LYP/6-31G(d,p) level of theory).

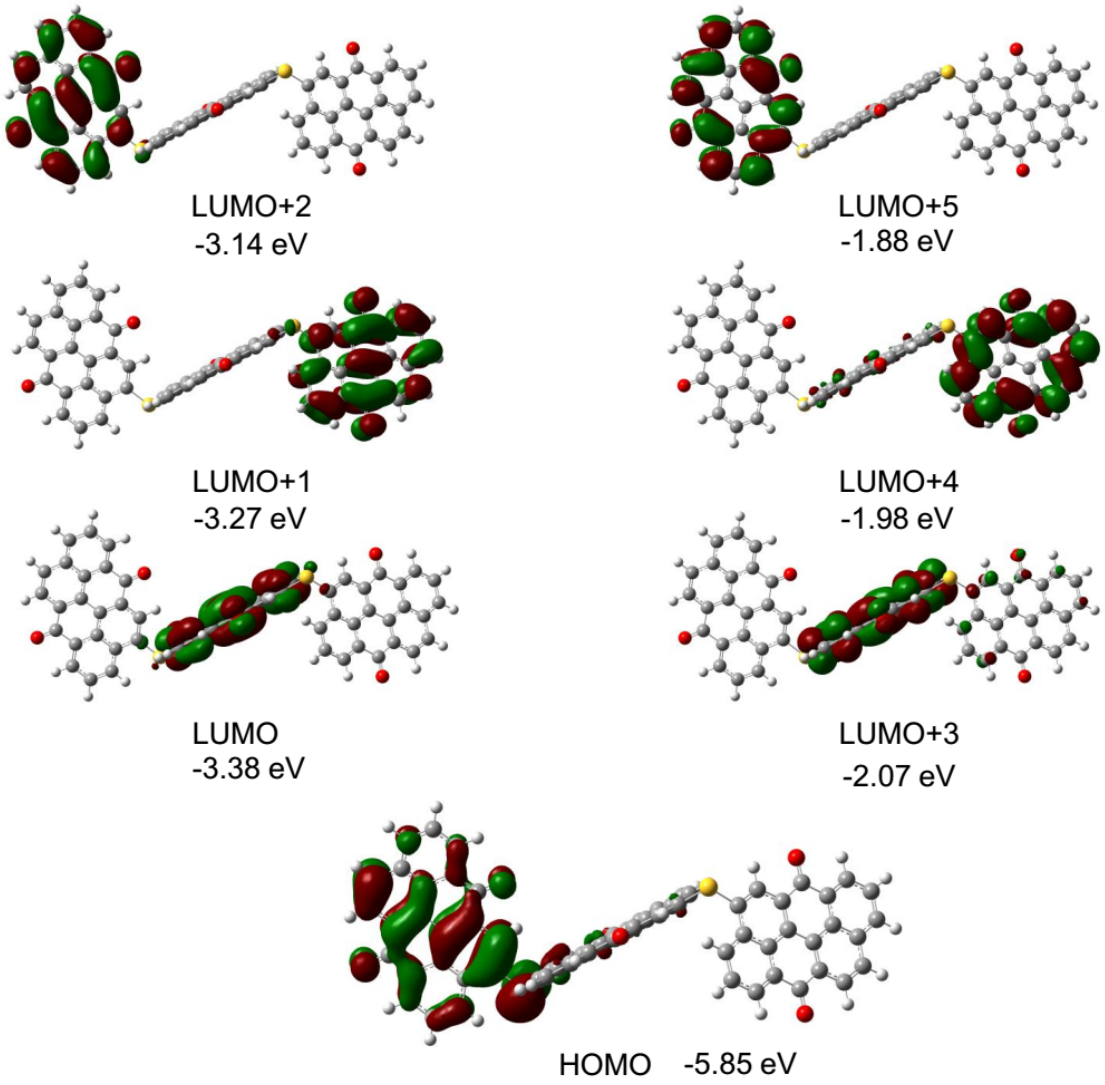

Figure S7. Frontier molecular orbital diagrams for **PATS** (B3LYP/6-31G(d,p) level of theory).

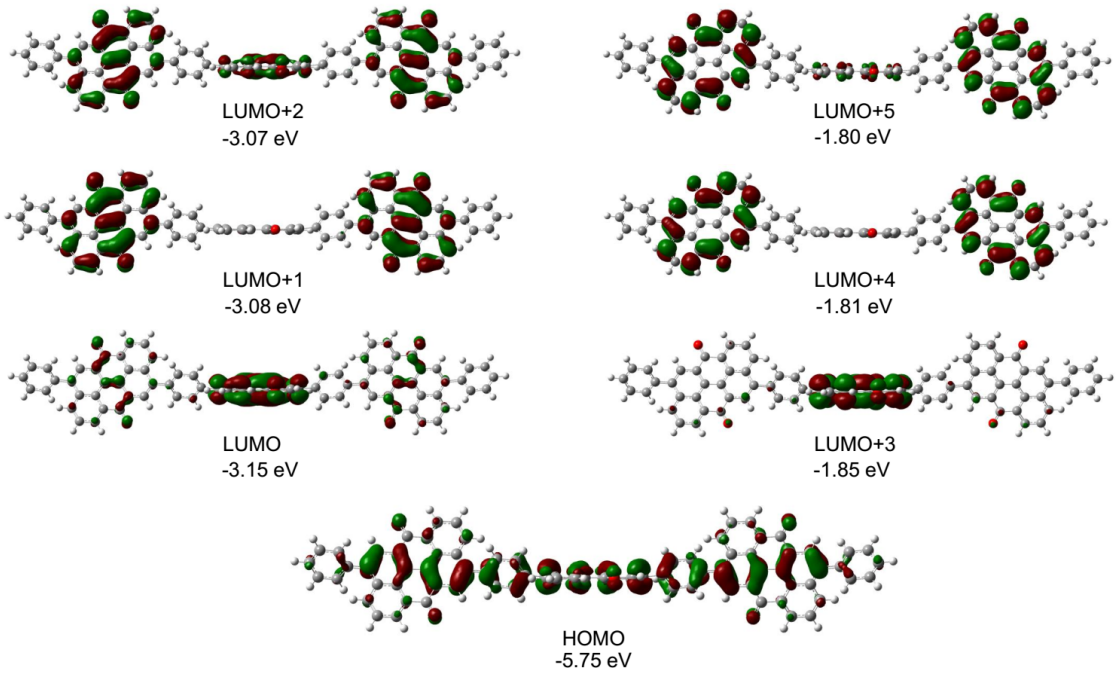

Figure S8. Frontier molecular orbital diagrams for **PAT-Ph** (B3LYP/6-31G(d,p) level of theory).

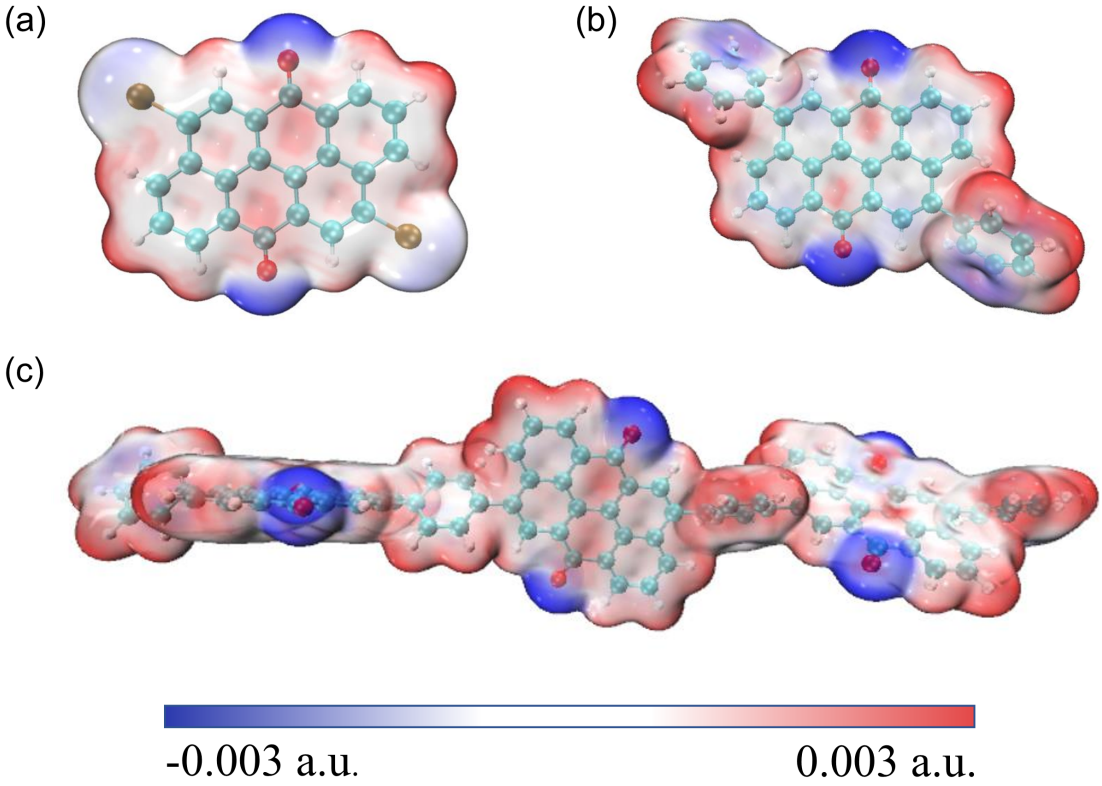

Figure S9. Molecular electrostatic potential (MESP) plots of (a) **VO3**, (b) **AT-Ph** and (c) **PAT-Ph**.

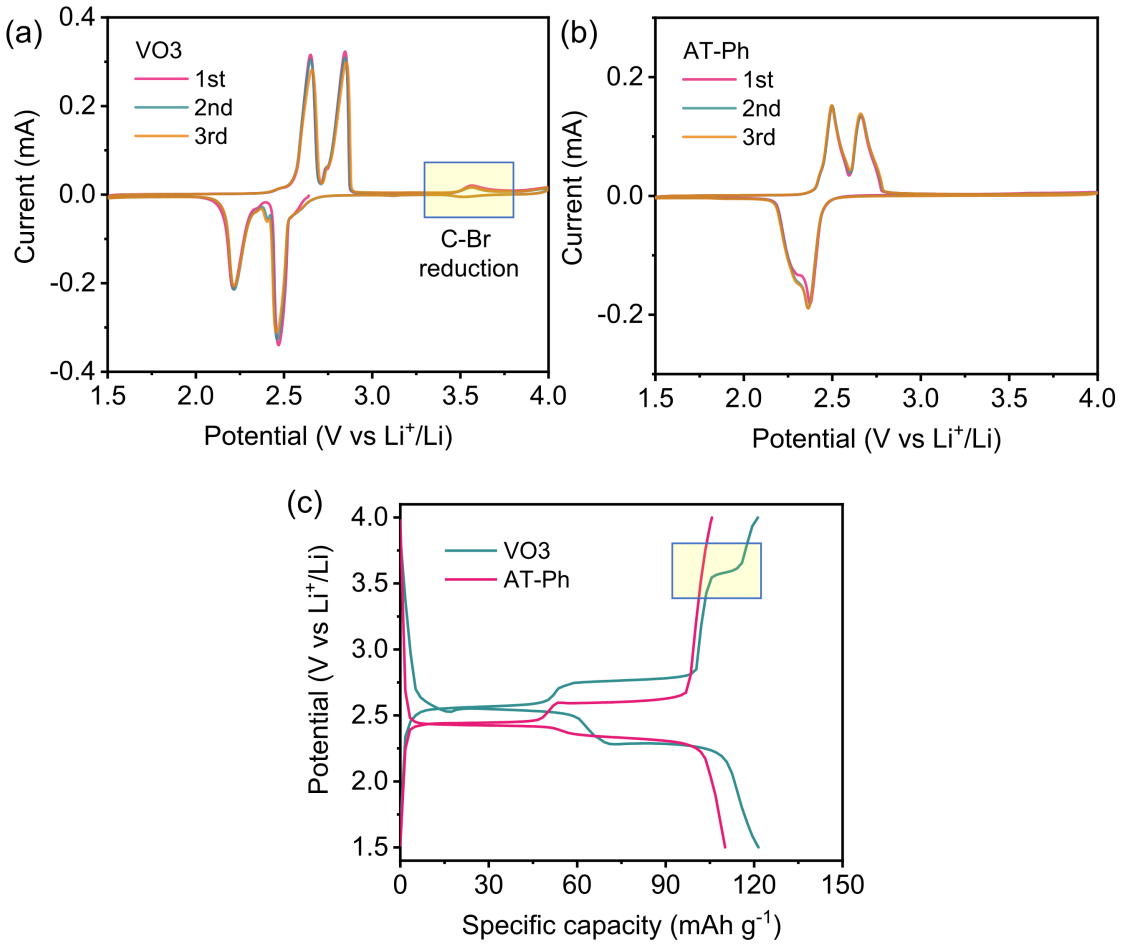

Figure S10. CVs of (a) **VO3**- and (b) **AT-Ph**-based electrodes in a battery configuration (6:3:1 active material/MWCNTs/PVDF) at 0.2 mV s^{-1}, (c) Galvanostatic charge-discharge profiles of **VO3** and **AT-Ph** at 0.1 A g^{-1}. The operation window is 1.5-4.0 V (vs Li/Li^+).

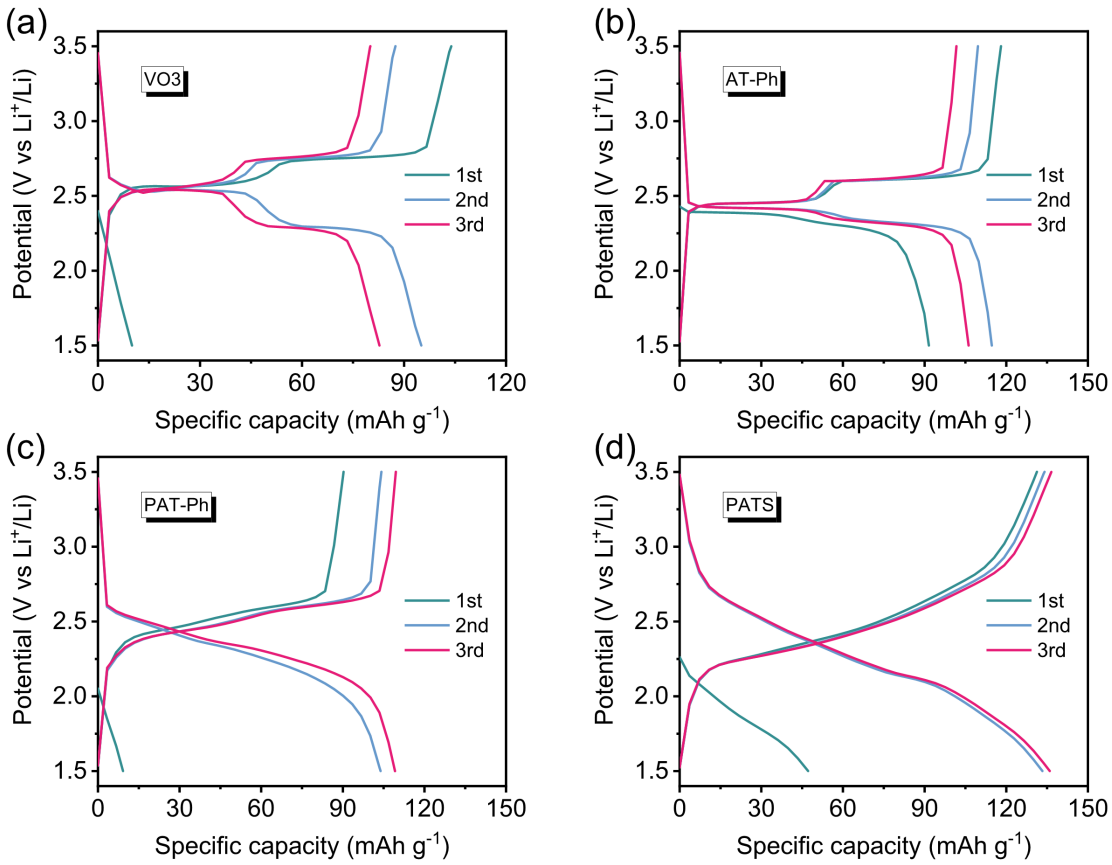

Figure S11. Galvanostatic charge-discharge profiles (1-3 cycles) at 0.2 A g^{-1} of (a) **VO3**, (b) **AT-Ph**, (c) **PAT-Ph** and (d) **PATS**.

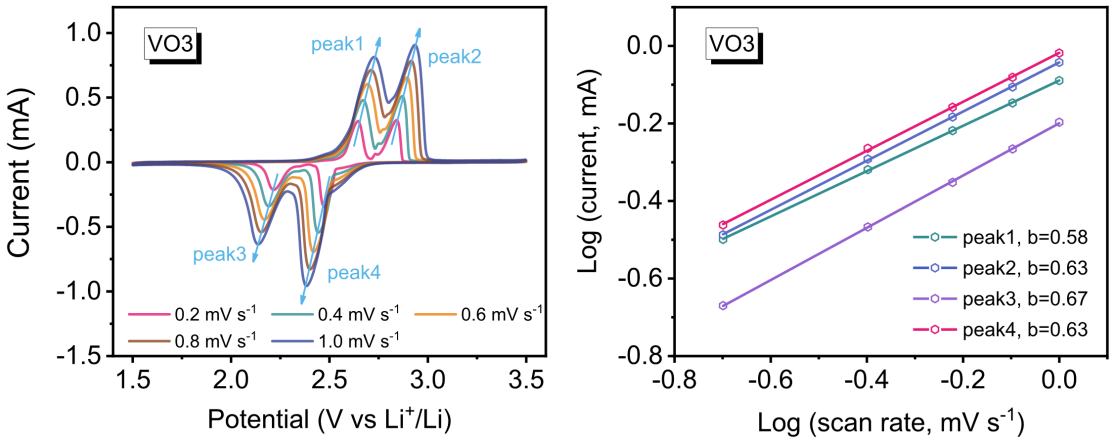

Figure S12. (left) CVs of the **VO3** electrode at different scan rates. (right) Log *i* versus log *v* plots of **VO3** to determine the b values of different peaks.

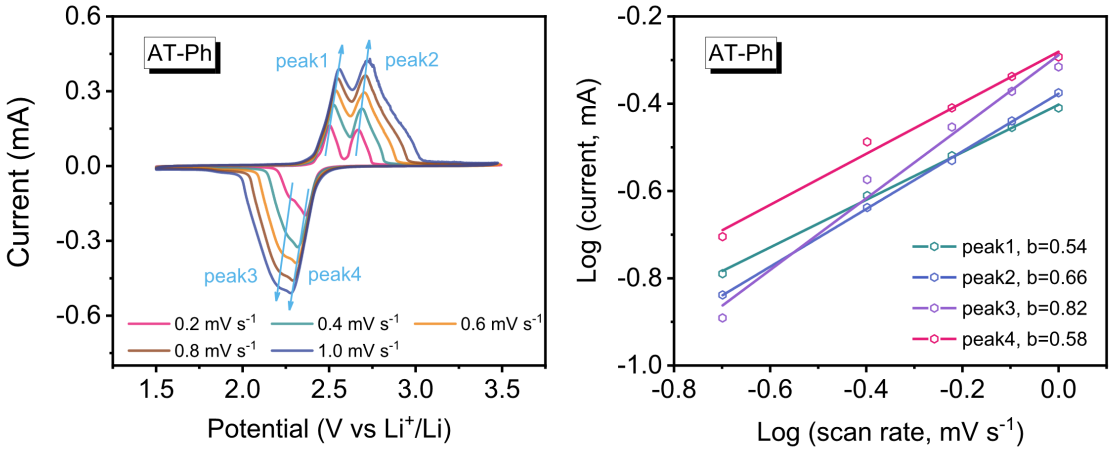

Figure S13. (left) CVs of the **AT-Ph** electrode at different scan rates. (right) Log *i* versus log *v* plots of **AT-Ph** to determine the b values of different peaks.

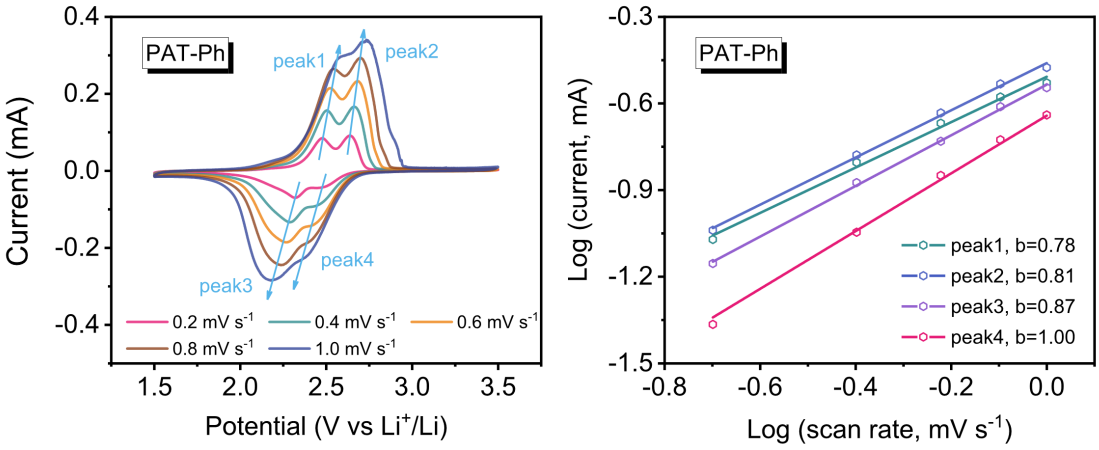

Figure S14. (left) CVs of the **PAT-Ph** electrode at different scan rates. (right) Log *i* versus log *v* plots of **PAT-Ph** to determine the b values of different peaks.

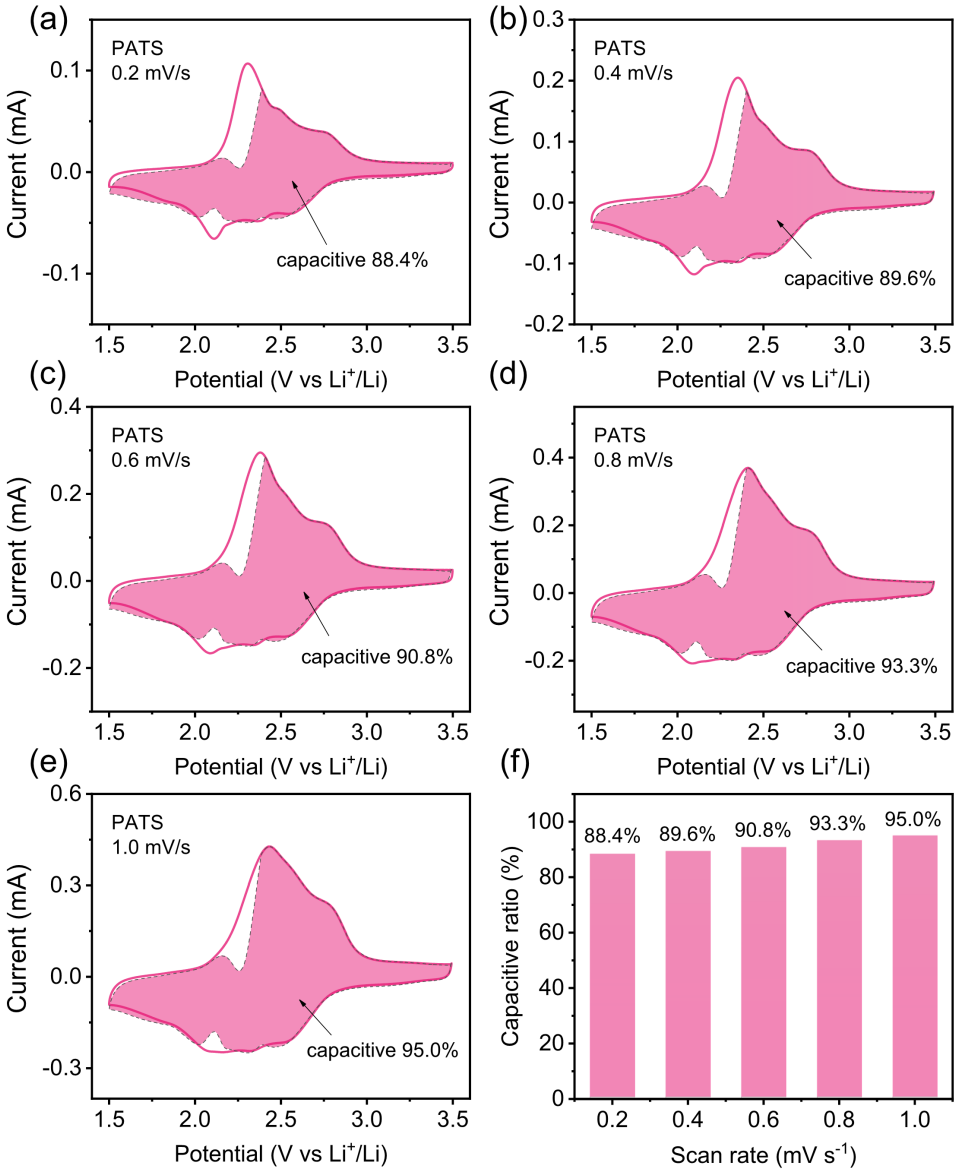

Figure S15. (a-e) Capacitive contribution of **PATS** in CV at 0.2, 0.4, 0.6, 0.8, 1.0 mV s^{-1}. (d) Capacitive contributions (in percentage) of **PATS** at different scan rates.

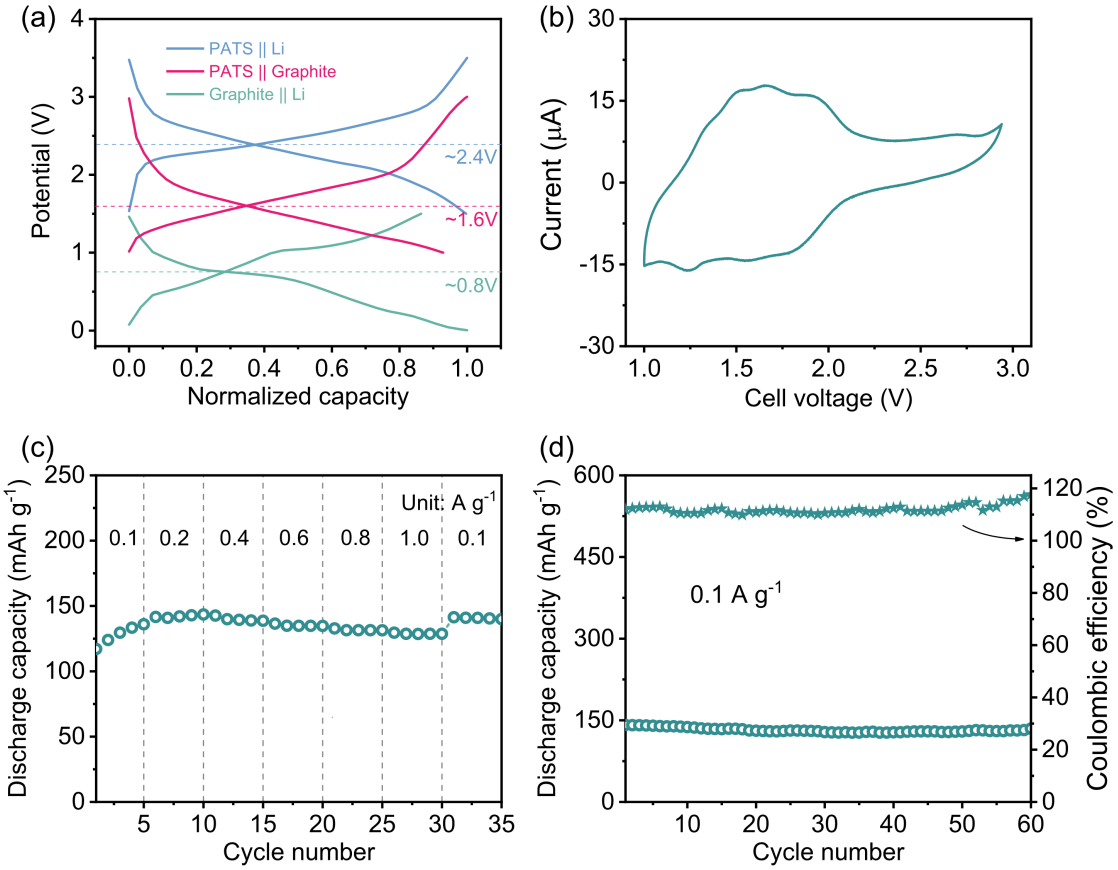

Figure S16. Full battery performance (**PATS** cathode and graphite anode) with 2M LiTFSI in G4 as electrolyte. (a) Normalized charge-discharge profiles of PATS || Li, graphite || Li and PATS || graphite. (b) CV of the full battery at 0.2 mV s^{-1}. (c) Rate performance at different current densities. (d) Cycling performance at 0.1 A g^{-1}.

When using 2M LiTFSI in G4 as the electrolyte, the voltage of graphite in the half cell is about 0.8V, resulting in an output voltage of ~1.6V for the **PATS** || graphite full cell. The Coulomb efficiencies are much higher than 100% during cycling, possibly due to the graphite composite being unstable in this electrolyte. Therefore, we choose 1M $LiPF_6$ in EC/DMC/EMC (1:1:1, v/v/v) as the electrolyte, to sacrifice a small amount of capacity to maintain battery stability when doing tests of **PATS** electrodes in full batteries.

Table S2. Cycling performance comparison of current work and other organic electrodes.

Chemical Structure	C_{theor} (mAh g^{-1})	Electrode Composition	Voltage Range (V vs Li/Li^+)	Electrolyte	Capacity, Capacity Retention	Ref.
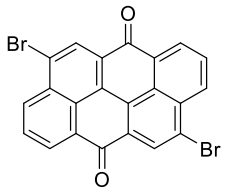 VO3	115	active material: MWCNTs: PVDF=6:3:1	1.5-3.5	2M LiTFSI in G4	40 mAh g^{-1}, 42 % (0.2 A g^{-1} after 300 cycles)	This work
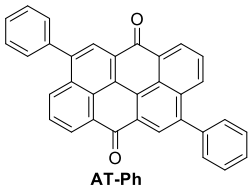 AT-Ph	117	active material: MWCNTs: PVDF=6:3:1	1.5-3.5	2M LiTFSI in G4	11 mAh g^{-1}, 10 % (0.2 A g^{-1} after 300 cycles)	This work
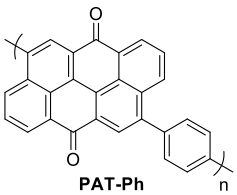 PAT-Ph	141	active material: MWCNTs: PVDF=6:3:1	1.5-3.5	2M LiTFSI in G4	84 mAh g^{-1}, 81 % (0.2 A g^{-1} after 300 cycles)	This work
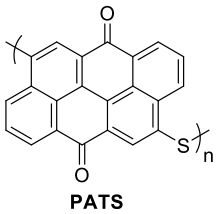 PATS	159	active material: MWCNTs: PVDF=6:3:1	1.5-3.5	2M LiTFSI in G4	132 mAh g^{-1}, 99 % (0.2 A g^{-1} after 300 cycles)	This work
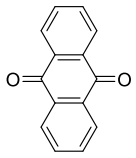 AQ	257	active materials: Ketjenblack EC-600JD: PTFE=6:3:1	1.5-3.0	1 M LiTFSI in DOL/DME (2:1, v/v)	~45 mAh g^{-1}, 17.8 % (0.2C after 100 cycles)	S4
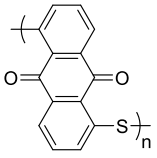 PAQS	225	active materials: Ketjenblack EC-600JD: PTFE=6:3:1	1.5-3.0	1 M LiTFSI in DOL/DME (2:1, v/v)	~210 mAh g^{-1}, 98.4 % (0.2C after 100 cycles)	S4
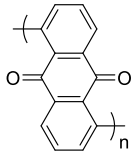 P15AQ	260	active materials: Ketjenblack EC-600JD: PTFE=6:3:1	1.5-3.0	1 M LiTFSI in DOL/DME (2:1, v/v)	~160 mAh g^{-1}, 67.6 % (0.2C after 100 cycles)	S4

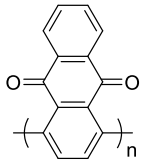 P14AQ	260	active materials: Ketjenblack EC-600JD: PTFE=6:3:1	1.5-3.0	1 M LiTFSI in DOL/DME (2:1, v/v)	~260 mAh g^{-1}, 98.3 % (0.2C after 100 cycles)	S4
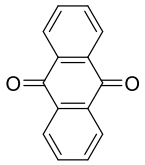 AQ	257	active materials: acetylene black: PTFE=4:4:2	1.4-3.5	1 M LiTFSI in DOL/DME (2:1, w/w)	~80 mAh g^{-1}, 37 % (50 mA g^{-1} after 50 cycles)	S5
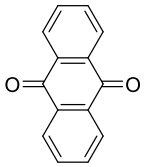 AQ	257	active materials: acetylene black: PTFE=4:4:2	1.4-3.5	1 M $LiClO_4$ in EC/DMC (1:1, v/v)	~100 mAh g^{-1}, 40 % (50 mA g^{-1} after 50 cycles)	S5
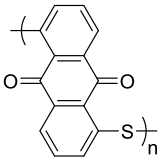 PAQS	225	active materials: acetylene black: PTFE=4:4:2	1.4-3.5	1 M LiTFSI in DOL/DME (2:1, w/w)	185 mAh g^{-1}, 93 % (50 mA g^{-1} after 40 cycles)	S5
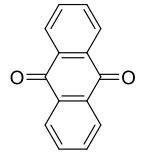 AQ	257	active materials: acetylene black: PVDF=7:2:1	1.5-4.0	1 M $LiPF_6$ in DMC	40 mAh g^{-1}, 15 % (0.1 C after 100 cycles)	S6
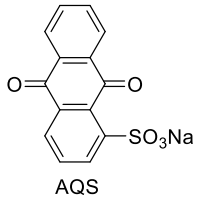 AQS	173	active materials: acetylene black: PVDF=7:2:1	1.5-4.0	1 M $LiPF_6$ in DMC	~75 mAh g^{-1}, 50 % (0.1 C after 100 cycles)	S6
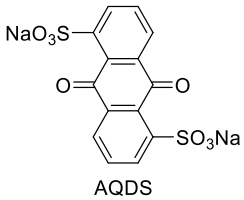 AQDS	130	active materials: acetylene black: PVDF=7:2:1	1.5-4.0	1 M $LiPF_6$ in DMC	120 mAh g^{-1}, 100 % (0.1 C after 100 cycles)	S6
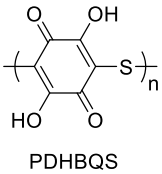 PDHBQS	315	active materials: acetylene black: PVDF=6:3:1	1.5-3.6	1 M $LiPF_6$ in EC/DMC (1:1, v/v)	184 mAh g^{-1}, 73.8 % (15 mA g^{-1} after 100 cycles)	S7

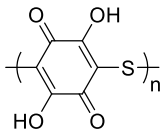 PDHBQS	315	active materials: conductive: PTFE=6:3:1	1.5-3.5	1 M LiTFSI in DOL/DME (1:1, weight)	~135 mAh g^{-1}, 89 % (250 mA g^{-1} after 500 cycles)	S8
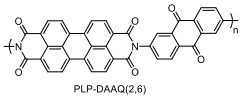 PLP-DAAQ(2,6)	270	active materials: super P carbon black: PVDF=6:3:1	1.5-3.5	1M LiTFSI in DOL/DME (2:1, w/w)	~100 mAh g^{-1}, 78 % (50 mA g^{-1} after 280 cycles)	S9
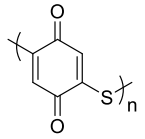 PBQS	388	active material: (Ketjenblack EC-600JD:PTFE= 6:3:1	1.5-4.0	1 M LiTFSI in DOL/DME (1:1, v/v)	212 mAh g^{-1}, 88 % (500 mA g^{-1} after 1000 cycles)	S10
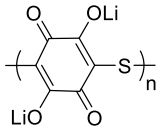 Li_2PDHBQS	294	active material: (Ketjenblack EC-600JD:PTFE= 6:3:1	1.5-3.0	1 M LiTFSI in DOL/DME (1:1, v/v)	215 mAh g^{-1}, 90 % (500 mA g^{-1} after 1500 cycles)	S11

All DFT calculations were carried out using the Gaussian 09 program package.[S9] The density functional theory (DFT) calculations were performed at the B3LYP/6-31G(d) level of theory.

Table S3. Cartesian coordinates for DFT-optimized structure of **VO3**.

C	-4.13632	2.31387	-0.11797
C	-4.4051	0.94459	-0.04031
C	-3.35059	0.03014	0.00639
C	-2.01948	0.49631	-0.02523
C	-1.79027	1.83474	-0.101
C	-2.85454	2.74941	-0.14768
C	-0.81952	-0.49631	0.02523
C	0.51159	-0.03014	-0.00639
C	0.79974	1.33782	-0.08405
C	-0.34802	2.34982	-0.13581
C	1.5661	-0.94459	0.04031
C	2.88845	-0.48598	0.00915
C	3.14336	0.84361	-0.06623
C	2.08667	1.76615	-0.11337
O	-0.11065	3.58365	-0.20577
C	-3.63873	-1.33782	0.08405
C	-2.49097	-2.34982	0.13582
C	-1.04872	-1.83474	0.10099
C	-5.72745	0.48598	-0.00915
C	-5.98235	-0.84361	0.06623
C	-4.92566	-1.76615	0.11338
C	0.01555	-2.74941	0.14767
C	1.29732	-2.31387	0.11796
O	-2.72835	-3.58365	0.20577
Br	-5.57471	3.56886	-0.1821
Br	2.73571	-3.56887	0.18209
H	-2.65123	3.79823	-0.20715
H	3.69801	-1.18473	0.04482
H	4.15504	1.19123	-0.08989
H	2.29735	2.81352	-0.17279
H	-6.537	1.18473	-0.04482
H	-6.99403	-1.19123	0.0899
H	-5.13634	-2.81352	0.1728
H	-0.18776	-3.79823	0.20714

Table S4. Cartesian coordinates for DFT-optimized structure of **AT-Ph**.

C	-3.58252	0.15914	-0.00869

C	-2.92389	-1.12272	-0.04385
C	-1.49329	-1.17758	-0.05095
C	-0.72704	0.029	-0.04888
C	-1.39668	1.25231	-0.05547
C	-2.80811	1.30168	-0.03384
C	0.72717	-0.02887	-0.04892
C	1.49343	1.17768	-0.05096
C	0.84081	2.44332	-0.07592
C	-0.64311	2.53399	-0.07032
C	2.92395	1.12285	-0.04388
C	3.63976	2.34692	-0.11193
C	2.98555	3.56346	-0.14306
C	1.58287	3.6137	-0.11391
O	-1.22527	3.61752	-0.07997
C	-0.8407	-2.44317	-0.07595
C	0.64322	-2.53388	-0.07048
C	1.3968	-1.25222	-0.0556
C	-3.63963	-2.34683	-0.11178
C	-2.98539	-3.56339	-0.14289
C	-1.58275	-3.61359	-0.11388
C	2.80821	-1.30155	-0.03397
C	3.58263	-0.159	-0.00864
O	1.22535	-3.61743	-0.08012
C	-5.06429	0.2945	0.05689
C	5.06412	-0.29445	0.05701
C	5.81425	0.31669	1.0765
C	7.1949	0.13658	1.15095
C	7.8524	-0.65609	0.20867
C	7.11875	-1.27245	-0.80593
C	5.73779	-1.09532	-0.87961
C	-5.81425	-0.31666	1.07646
C	-7.19493	-0.13681	1.15099
C	-7.85266	0.6557	0.20873
C	-7.11919	1.27202	-0.806
C	-5.73818	1.0951	-0.87977
H	-3.26977	2.28252	-0.0071
H	4.72218	2.31827	-0.15172
H	3.55864	4.4839	-0.19781
H	1.04888	4.55793	-0.13373
H	-4.72206	-2.31822	-0.15134
H	-3.55851	-4.48381	-0.19753
H	-1.0487	-4.55778	-0.13371
H	3.27006	-2.28234	-0.00734
H	5.30739	0.91527	1.82739

H	7.75585	0.60928	1.95193
H	8.92785	-0.79485	0.26693
H	7.62158	-1.89076	-1.54375
H	5.17126	-1.56969	-1.67528
H	-5.30737	-0.91516	1.82735
H	-7.75576	-0.60959	1.95201
H	-8.92812	0.79428	0.26716
H	-7.62208	1.89019	-1.54389
H	-5.17197	1.56946	-1.67564

Table S5. Cartesian coordinates for DFT-optimized structure of **PAT-Ph**.

C	16.54362	0.25164	0.00514
C	15.85429	-0.94975	-0.39402
C	14.42377	-0.98722	-0.34917
C	13.68685	0.16673	0.06083
C	14.38427	1.32328	0.40877
C	15.79592	1.35118	0.37685
C	12.23252	0.12793	0.10243
C	11.49523	1.28282	0.51057
C	12.17731	2.47252	0.89397
C	13.66144	2.54771	0.84413
C	10.06484	1.24771	0.54946
C	9.38097	2.39644	1.02709
C	10.06412	3.53643	1.40471
C	11.46512	3.58051	1.32639
O	14.26752	3.57318	1.14986
C	13.74167	-2.17807	-0.72987
C	12.25808	-2.25374	-0.67927
C	11.53537	-1.02855	-0.24581
C	16.53781	-2.09868	-0.87179
C	15.85486	-3.24046	-1.2445
C	14.45414	-3.28593	-1.16255
C	10.12315	-1.05442	-0.22027
C	9.37633	0.04768	0.14432
O	11.65066	-3.27875	-0.98489
C	18.02944	0.34771	0.03498
C	18.81045	-0.55585	0.77583
C	20.1969	-0.41901	0.83252
C	20.82929	0.62141	0.14978
C	20.06493	1.52825	-0.58571
C	18.67826	1.39421	-0.64052
C	3.58294	-0.38878	-0.09849
C	2.83495	-0.43501	-1.32991

C	1.40446	-0.4523	-1.28194
C	0.72729	-0.45293	-0.02301
C	1.48292	-0.45827	1.14908
C	2.89398	-0.4249	1.09732
C	-0.72725	-0.45275	0.02387
C	-1.40443	-0.45094	1.28279
C	-0.66287	-0.48057	2.49814
C	0.8236	-0.47711	2.48192
C	-2.83492	-0.43328	1.33075
C	-3.46164	-0.50079	2.60278
C	-2.72201	-0.5404	3.76911
C	-1.31922	-0.51804	3.71876
O	1.48261	-0.48844	3.52026
C	0.6629	-0.48277	-2.49726
C	-0.82357	-0.47892	-2.48105
C	-1.48288	-0.45886	-1.14821
C	3.46167	-0.50384	-2.60187
C	2.72203	-0.54426	-3.76816
C	1.31924	-0.52145	-3.71785
C	-2.89394	-0.4252	-1.09648
C	-3.58291	-0.388	0.0993
O	-1.48259	-0.49091	-3.51937
C	5.06725	-0.28584	-0.07163
C	-5.06721	-0.28503	0.07231
C	-5.74356	0.74969	0.7406
C	-7.12762	0.87198	0.65846
C	-7.89136	-0.03761	-0.09236
C	-7.21576	-1.0742	-0.75535
C	-5.83041	-1.1922	-0.67935
C	5.74352	0.74852	-0.74057
C	7.12758	0.87088	-0.6586
C	7.89138	-0.03826	0.09272
C	7.21585	-1.07447	0.75637
C	5.8305	-1.19255	0.68051
C	-9.37631	0.0482	-0.1441
C	-10.06493	1.24797	-0.54984
C	-11.49533	1.28291	-0.51113
C	-12.23253	0.12812	-0.10253
C	-11.53527	-1.02809	0.24635
C	-10.12304	-1.05381	0.22095
C	-13.68687	0.16676	-0.06112
C	-14.42369	-0.98709	0.34936
C	-13.74148	-2.17765	0.73074
C	-12.25787	-2.25317	0.68033

C	-15.85422	-0.94978	0.39402
C	-16.53763	-2.09855	0.87234
C	-15.85458	-3.24004	1.24572
C	-14.45385	-3.28539	1.16392
O	-11.65035	-3.27796	0.98652
C	-12.17752	2.47235	-0.89517
C	-13.66166	2.54736	-0.84556
C	-14.38439	1.32304	-0.40971
C	-9.38116	2.39658	-1.0279
C	-10.06441	3.53631	-1.40612
C	-11.46542	3.58023	-1.32802
C	-15.79605	1.35077	-0.378
C	-16.54365	0.25131	-0.00586
O	-14.26784	3.57261	-1.15186
C	-18.02948	0.34714	-0.03605
C	-18.8102	-0.55703	-0.77647
C	-20.19665	-0.42042	-0.83358
C	-20.82935	0.62036	-0.15167
C	-20.06529	1.5278	0.58339
C	-18.67861	1.394	0.6386
H	16.28153	2.26942	0.68817
H	8.30072	2.36808	1.10709
H	9.51533	4.39911	1.76962
H	12.02119	4.46739	1.61154
H	17.61781	-2.0685	-0.95365
H	16.40354	-4.10359	-1.60857
H	13.89835	-4.17383	-1.44512
H	9.63843	-1.97235	-0.53425
H	18.32449	-1.3537	1.32931
H	20.78245	-1.12154	1.41838
H	21.90923	0.72626	0.19364
H	20.548	2.34078	-1.12044
H	18.08744	2.09694	-1.22032
H	3.42402	-0.39238	2.04285
H	-4.54358	-0.53498	2.65319
H	-3.22801	-0.59612	4.72794
H	-0.71938	-0.54255	4.62246
H	4.54359	-0.53847	-2.65227
H	3.22801	-0.601	-4.72694
H	0.71939	-0.54658	-4.62153
H	-3.42397	-0.39337	-2.04205
H	-5.17738	1.47526	1.31653
H	-7.62493	1.67443	1.19467
H	-7.78445	-1.7877	-1.34382

H	-5.33057	-2.00225	-1.20169
H	5.17727	1.47377	-1.31684
H	7.62484	1.67299	-1.19535
H	7.7846	-1.78761	1.34522
H	5.33071	-2.00229	1.20337
H	-9.63824	-1.97154	0.53541
H	-17.61765	-2.06847	0.95412
H	-16.40318	-4.10305	1.61019
H	-13.89797	-4.17307	1.447
H	-8.30089	2.36835	-1.10771
H	-9.51569	4.39889	-1.77135
H	-12.02158	4.4669	-1.61365
H	-16.28174	2.26878	-0.68986
H	-18.32399	-1.35517	-1.3293
H	-20.78197	-1.12343	-1.4191
H	-21.90929	0.72503	-0.19585
H	-20.5486	2.34062	1.11747
H	-18.08803	2.0972	1.21808

Table S6. Cartesian coordinates for DFT-optimized structure of **PATS**.

C	-5.26277142	0.10262488	-3.18134555
C	-5.18560606	-1.27213303	-3.42125837
C	-4.03396287	-1.97715903	-3.06465725
C	-2.95507285	-1.29512053	-2.46406192
C	-3.05995150	0.04301619	-2.24452243
C	-4.22040992	0.74651049	-2.60483113
C	-1.65604860	-2.05095304	-2.05307878
C	-0.57706874	-1.36855503	-1.45308560
C	-0.63582672	0.00848977	-1.20703248
C	-1.89281006	0.79205312	-1.59410672
C	0.57395779	-2.07348012	-1.09550207
C	1.64750326	-1.39991879	-0.50080712
C	1.56812370	-0.06590331	-0.27239146
C	0.41290333	0.64650087	-0.62954174
O	-1.96590057	2.03022009	-1.38159813
C	-3.97444765	-3.35393842	-3.31242895
C	-2.71763439	-4.13783073	-2.92460445
C	-1.55122261	-3.38926942	-2.27203979
C	-6.25832863	-1.94532573	-4.01780738
C	-6.17773722	-3.27891607	-4.24893536
C	-5.02232969	-3.99136710	-3.89217786
C	-0.39145192	-4.09303098	-1.90924858
C	0.65034262	-3.44848487	-1.33242115

O	-2.64416646	-5.37583005	-3.13821762
C	3.52789709	-3.27071050	-0.98815398
C	4.24900508	-3.18362445	-2.18213528
C	5.35487828	-2.33485612	-2.26694687
C	5.73555751	-1.56925249	-1.14500439
C	5.01398503	-1.67627534	0.00291020
C	3.90452561	-2.53300001	0.08289492
C	6.96243865	-0.61075403	-1.20571185
C	7.34103600	0.15693298	-0.08454070
C	6.63053536	0.08250045	1.11960348
C	5.41955683	-0.84813030	1.22591397
C	8.44394305	1.00876890	-0.17035902
C	8.82225669	1.77354793	0.93954096
C	8.11929757	1.68482844	2.09544994
C	7.01066073	0.82908181	2.18653587
O	4.76835860	-0.93110459	2.29947829
C	6.06613483	-2.26135719	-3.47081585
C	7.28055996	-1.33464069	-3.57554055
C	7.68577948	-0.50560904	-2.35282288
C	3.86706438	-3.94398141	-3.29362991
C	4.57078083	-3.85636037	-4.44930918
C	5.68341215	-3.00534039	-4.53878082
C	8.79612713	0.35056585	-2.43218529
C	9.16671144	1.09457728	-1.36306743
O	7.93446824	-1.25513021	-4.64778005
S	10.57185665	2.18132374	-1.47305457
S	2.11607511	-4.34890427	-0.87560310
C	11.29716116	2.36716775	0.14167143
C	10.86144495	3.39102276	0.98694526
C	11.42732091	3.53497408	2.25513646
C	12.43755716	2.64422504	2.67440322
C	12.84174159	1.65855110	1.82859771
C	12.26906695	1.51904998	0.55386254
C	13.08961594	2.77586599	4.08328786
C	14.09982011	1.88527641	4.50292264
C	14.55087562	0.85474673	3.66940215
C	13.93840337	0.68703551	2.27616533
C	14.66473791	2.02852892	5.77198037
C	15.66755396	1.14701512	6.19227367
C	16.08913788	0.15686551	5.36760799
C	15.52413513	0.00906831	4.09132869
O	14.32915596	-0.23319829	1.51194092
C	10.97698907	4.56623667	3.08830127
C	11.58928198	4.73356902	4.48137441

C	12.68529487	3.76141921	4.92887950
C	9.85881223	4.27306506	0.56659989
C	9.43877097	5.26457286	1.39046268
C	10.00449837	5.41279695	2.66624020
C	13.25697532	3.90038143	6.20371987
C	14.22703253	3.05123544	6.61764434
O	11.19878025	5.65390577	5.24563731
H	-6.14407336	0.64544400	-3.45279351
H	-4.28146466	1.79910273	-2.42255669
H	2.53073440	-1.93800087	-0.22653787
H	2.39017120	0.44621272	0.18240306
H	0.35903870	1.69909128	-0.44531504
H	-7.14187020	-1.40745417	-4.29141099
H	-6.99901638	-3.79067538	-4.70557971
H	-4.96769919	-5.04355875	-4.07855597
H	-0.33054675	-5.14592059	-2.08984980
H	3.35231311	-2.60306442	0.99676842
H	9.66642753	2.42795067	0.87561443
H	8.41116864	2.27001619	2.94232197
H	6.46195240	0.76510454	3.10284363
H	3.01974123	-4.59437007	-3.23110021
H	4.27647152	-4.43880669	-5.29722843
H	6.23294850	-2.94297075	-5.45473006
H	9.35266145	0.41586545	-3.34382071
H	12.60279269	0.73714425	-0.09583104
H	16.10135124	1.25468044	7.16441539
H	16.85629559	-0.51511528	5.69138108
H	15.86302542	-0.77521160	3.44727326
H	9.42395605	4.16465188	-0.40501345
H	8.67230902	5.93722654	1.06640997
H	9.66678353	6.19804454	3.30983525
H	12.92363352	4.68294043	6.85282464
H	14.65786251	3.16300744	7.59065967

References

[1] Z. Song, Y. Qian, M. L. Gordin, D. Tang, T. Xu, M. Otani, H. Zhan, H. Zhou, D. Wang, *Angew. Chem. Int. Ed.* **2015**, *54*, 13947-13951.

[2] Z. Song, H. Zhan, Y. Zhou, *Chem. Commun.* **2009**, 448-450.

[3] W. Wan, H. Lee, X. Yu, C. Wang, K.-W. Nam, X.-Q. Yang, H. Zhou, *RSC Adv.* **2014**, *4*, 19878-19882.

[4] K. Liu, J. Zheng, G. Zhong, Y. Yang, *J. Mater. Chem.* **2011**, *21*, 4125-4131.

[5] K. Amin, Q. Meng, A. Ahmad, M. Cheng, M. Zhang, L. Mao, K. Lu, Z. Wei, *Adv. Mater.* **2018**, *30*, 1703868.

[6] M.-H. Jung, R. V. Ghorpade, *J. Electrochem. Soc.* **2018**, *165*, A2476-A2482.

[7] Z. Song, Y. Qian, T. Zhang, M. Otani, H. Zhou, *Adv. Sci.* **2015**, *2*, 1500124.

[8] Z. Song, Y. Qian, X. Liu, T. Zhang, Y. Zhu, H. Yu, M. Otani, H. Zhou, *Energy Environ. Sci.* **2014**, *7*, 4077-4086.

[9] M. J. Frisch, G. W. Trucks, H. B. Schlegel, G. E. Scuseria, M. A. Robb, J. R. Cheeseman, G. Scalmani, V. Barone, B. Mennucci, G. A. Petersson, H. Nakatsuji, M. Caricato, X. Li, H. P. Hratchian, A. F. Izmaylov, J. Bloino, G. Zheng, J. L. Sonnenberg, M. Hada, M. Ehara, K. Toyota, R. Fukuda, J. Hasegawa, M. Ishida, T. Nakajima, Y. Honda, O. Kitao, H. Nakai, T. Vreven, J. A. Montgomery, Jr., J. E. Peralta, F. Ogliaro, M. Bearpark, J. J. Heyd, E. Brothers, K. N. Kudin, V. N. Staroverov, T. Keith, R. Kobayashi, J. Normand, K. Raghavachari, A. Rendell, J. C. Burant, S. S. Iyengar, J. Tomasi, M. Cossi, N. Rega, J. M. Millam, M. Klene, J. E. Knox, J. B. Cross, V. Bakken, C. Adamo, J. Jaramillo, R. Gomperts, R. E. Stratmann, O. Yazyev, A. J. Austin, R. Cammi, C. Pomelli, J. W. Ochterski, R. L. Martin, K. Morokuma, V. G. Zakrzewski, G. A. Voth, P. Salvador, J. J. Dannenberg, S. Dapprich, A. D. Daniels, O. Farkas, J. B. Foresman, J. V. Ortiz, J. Cioslowski, and D. J. Fox, **2010**, Gaussian 09, Revision B.01 (*Gaussian, Inc, Wallingford CT*).